Indian Journal of Experimental Biology
Vol. 63, March 2025, pp. 239-251
DOI: 10.56042/ijeb.v63i03.11618

Immobilized *Scenedesmus regularis* for enhanced biosorption of zinc oxide nanoparticles

Neha Shrivastava, Vikas Shrivastava, Vinay Dwivedi & Anurag Jyoti*

Amity Institute of Biotechnology, Amity University Madhya Pradesh, Maharajpura Dang, Gwalior, Madhya Pradesh, India

Received 22 July 2024; revised 28 January 2025

Zinc oxide (ZnO) nanoparticles are among the most widely used nanoparticles as ingredients in various products. These nanoparticles often enter the water bodies through industrial discharge and other means. Once they reach into the water, they remain there for longer time and show toxicity to aquatic flora, fauna and even human beings upon exposure. Despite their potential hazards, the removal of nanoparticles from the environment has not been extensively studied, making it a pressing issue for both human health and the environment. Driven by this need, the present study has undertaken to develop a biosorption method using immobilized *Scenedesmus regularis* green microalgae to remove ZnO nanoparticles. In this research, environmentally isolated microalgae were characterized using 18S rRNA gene sequencing. The ZnO nanoparticles were chemically synthesized and characterized through Fourier transform infrared spectroscopy (FTIR), transmission electron microscopy (TEM), and X-ray diffraction (XRD). Batch sorption experiments were conducted to demonstrate the efficiency of *Scenedesmus regularis* in absorbing ZnO nanoparticles under various conditions. Statistical analysis using one-way ANOVA was conducted to compare conditions before and after biosorption. The 18S rRNA gene sequencing confirmed that the isolated species was *Scenedesmus regularis*. ICPMS results showed that the immobilized *Scenedesmus regularis* microalgal biomass, encapsulated in sodium alginate beads, effectively removed 82.53% of ZnO nanoparticles at an initial concentration of 80 mg/L within 3 h. FTIR analysis revealed that carboxyl, amine, hydroxyl, sulfate, and sulfonate functional groups on the *Scenedesmus regularis* cell wall played a significant role in binding ZnO nanoparticles. Additionally, SEM-EDX imaging confirmed the attachment of ZnO nanoparticles to the surface of *Scenedesmus regularis* cells. The results of the adsorption/desorption studies showed that the *Scenedesmus regularis* biosorbent could be regenerated many times with no extensive reduction in ZnO nanoparticles' adsorption percentage. Present study exposed to provide an alternative to conventional wastewater treatment techniques. This research focuses that *Scenedesmus regularis* as a biosorbents appeared to be more efficient to uptake of ZnO nanoparticles and has a potential to be reused for multiple cycles of nanoparticles uptake. The study aims to eliminate toxic nanoparticles from aqueous environments through microalgae biosorption. This method is efficient, natural, safe, eco-friendly, and more economical.

Keywords: Adsorption, Desorption, Nanoparticles, Matrix-coupled, *Scenedesmus regularis*

Rapid industrialization near water bodies poses severe health implications in aquatic ecosystem[1]. Various industries, such as those involved in construction, electrical equipment, plumbing, roofing, industrial machinery (including mining and heat exchangers), pharmaceuticals, wood production, metal production, and phosphate fertilizer production, discharge substantial amounts of chemical pollutants in nearby rivers[2,3]. Industries utilizing nanoparticles are especially hazardous as these particles are non-biodegradable and soluble in aquatic environments[4]. Nowadays, metal oxide nanoparticles have found increasing applications in numerous commercial and industrial products. ZnO nanoparticles are widely used in cosmetics, consumer goods, and modern sunscreens due to their strong ultraviolet absorption properties[5]. Research has highlighted the large-scale production of ZnO nanoparticles, ranging from 100 to 1,000 times more than other nanomaterials, which are likely to enter water bodies through industrial sewage[6]. This unintentional exposure affects both humans and the environment, negatively impacting the survival and growth of organisms[7]. These nanoparticles are readily absorbed by vegetables and marine species due to their high solubility in water. The toxicity of nanoparticles arises from their ability to internalize into cells, causing cytotoxicity and genotoxicity. Therefore, preventing the dispersal of toxic nanomaterials into water bodies and food chains and removing them from effluents before disposal is crucial for environmental health, management, and economics.

*Correspondence:
Phone: +91 78988 05402 (Mob.)
E-mail: ajyoti@gwa.amity.edu

Reducing nanoparticles toxicity remains a significant challenge for developing countries. The high costs of waste management often lead industries to increase the discharge of toxic nanoparticles into the environment[8].

Biosorption is a physicochemical process that uses biological materials. This technology is designed to bind and remove toxic metals from aqueous solutions, soil and air. Biosorption is an emerging, innovative, economical, and eco-friendly technology. Generally, the mechanism of biosorption is based on physico-chemical interactions between functional groups and metal ions present on the surface of biosorbent. Biosorption of metals has been attributed to the presence of various functional groups on the microalgal cell wall such as proteins, lipids and polysaccharides. They contain amino, carboxyl, imidazole, phosphoryl, sulfydryl, sulfate, phenol, thioether, carbonyl, amide hydroxyl moieties, depending on the biosorbents nature[9]. Biosorption offers several advantages over conventional methods: low cost, high efficiency, minimal chemical or biological sludge disposal, the ability to regenerate biosorbents, high competence in detoxifying effluents, and no nutrient requirements. Microalgae can uptake, accumulate, and concentrate nanoparticles and hazardous components from aqueous solutions in significant amounts[10,11]. While many studies have explored the uptake of heavy metals by plants and algae, their efficiency remains limited[12]. Few studies have investigated nanoparticles uptake by plants, with insignificant results[13]. Notably, there are no reports on nanoparticles uptake by algae.

Present study exposed to provide an alternative to conventional wastewater treatment techniques. This research focuses that *Scenedesmus regularis* as a biosorbents appeared to be more efficient to uptake of ZnO nanoparticles and has a potential to be reused for multiple cycles of nanoparticles uptake. The study aims to eliminate toxic nanoparticles from aqueous environments through microalgae biosorption. This method is efficient, natural, safe, eco-friendly, and more economical.

Materials and Methods

Collection of samples and growth condition

Eutrophic water samples were collected from Baija Taal in Gwalior, Madhya Pradesh, India (26.2082° N, 78.1711° E) where the temperature ranged from 33°C to 35°C. To isolate the *Scenedesmus regularis*, enrichment was done by inoculating 100 mL of the sterilized fresh BG-11 broth medium, having *p*H of 7.4. The standard protocol for the isolation and purification of *Scenedesmus* sp. was followed[14]. Isolated microalgae were cultured in batch mode for 24 days under optimized laboratory conditions. The maximum absorbance was recorded at 682 nm[15]. Scenedesmus is a non-motile colonial alga composed of 2, 4, or 8 elongated cells that are grouped together. Through multiple purification experiments, axenic cultures were confirmed by examining them under an inverted microscope at 40 × magnification. All pure cultures were maintained in BG-11 broth medium as well as on BG-11 agar plates at 27.0 ± 2.0°C temperatures with a 16:8-h light-dark cycle under fluorescent light[16]. After accomplishing significant growth, obtained dry weight (g/L) was 1.38 g/L for biosorption studies.

Physical and molecular characterization

Microscopically identified isolates were further reconfirmed using a reference strain as a positive control. To achieve molecular-based authentication of the isolated *Scenedesmus regularis* samples, PCR, targeting18S rRNA gene followed by sequencing were performed. Morphologically confirmed samples of green microalgae were sent for PCR and 18S rRNA gene sequencing to Barcode Biosciences, Bengaluru, Karnataka and result was obtained via Sanger sequencing. Universal eukaryotic primers NS1 (5'-GTAGTCATATGCTTGTCTC-3') and NS4 (5'-CTTCCGTCAATTCCTTTAAG-3') were used.

Synthesis of zinc oxide nanoparticles

Zinc oxide nanoparticles were synthesized using the direct precipitation method with 0.2 M zinc nitrate ($Zn(NO_3)_2 \cdot 6H_2O$) and 0.4 M potassium hydroxide (KOH) as precursors. Potassium hydroxide added drop wise to the zinc nitrate solution at room temperature with constant stirring on a magnetic stirrer for 3 h. Upon completion of the reaction, a white precipitate was formed[17]. This precipitate was washed 4-5 times with ethanol to remove impurities and then dried at approximately 80°C for 24 h (Fig. 1)[18].

Characterization of zinc oxide nanoparticles

The presence of functional groups in the zinc oxide nanoparticles was determined using Fourier transform infrared spectroscopy (FTIR) (Perkin Elmer, Spectrum Two), with spectra recorded in the range of 450-4000 cm^{-1}. The UV-Vis absorption spectrum of the zinc oxide nanoparticles was recorded over the wavelength range of 200-600 nm to confirm the

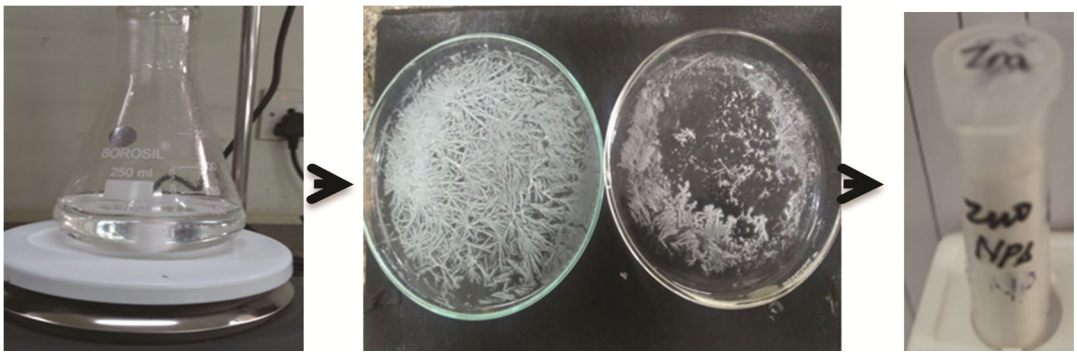

Fig. 1 — (A) Chemical synthesis of ZnO nanoparticles; (B&C) Dried nanoparticles

presence of nanoparticles[19]. To categorize the crystal phases and determine the crystallite size of each phase, powdered x-ray diffraction (XRD) analysis was utilized. Transmission electron microscopy (TEM) (JEOL, JEM-1230) was conducted to confirm the actual size of the particles, distribution of the growth pattern, and crystallites, operating at an acceleration voltage of 120 kV.

Preparation of biosorbent

The wet biomass of the microalgal cell suspension was collected by centrifugation for 15 min at 5000 rpm[20]. The resulting pellets were washed 2-3 times with distilled water to remove impurities, and the biomass was then dried for 12 h at 80°C in an oven. After drying, the algae were crushed to a particle size range of 100-500 µm using a mortar and pestle[21].

Immobilization of *Scenedesmus regularis biomass*

The biosorption capacity of *Scenedesmus regularis* biomass for zinc oxide nanoparticles uptake from aqueous solution was assessed using immobilized *Scenedesmus regularis* biomass in sodium alginate beads. A 4% sodium alginate solution was prepared by dissolving 4 g of sodium alginate into 100 mL of distilled water, followed by continuous stirring for 30 min at 60°C for better dissolution and sterilization. After cooling, five different nominal concentrations (0.5, 1, 1.5, 2, and 3 g/L) of dried *Scenedesmus regularis* biomass powder were added while stirring at room temperature for 5 min. Spherical beads were formed by dropping the alginate-algal mixture through a 3 mL syringe into a cold, sterile 2% CaCl2 solution in distilled water at room temperature under sterile conditions and gentle stirring. The resulting beads were washed several times with autoclaved distilled water to remove any unreacted CaCl2 from their surfaces and then stored overnight at 4°C in autoclaved distilled water to stabilize and harden the beads. Sodium alginate beads without the incorporation of *Scenedesmus regularis* biomass were also prepared using the same procedure and served as control[22].

Bath sorption procedures

Biosorption experiments were proficient to study the adsorption of zinc oxide nanoparticles (ZnO NPs) using a batch system. This study aimed to investigate the effects of various parameters on the sorption process, including initial *p*H, biosorbent dosage, contact time, and temperature. The initial concentration of ZnO NPs in the aqueous solution, ranging from 20 to 100 mg/L, was adjusted by dilution with deionized water (Rankem). The experiments were carried out under varying conditions of *p*H (4, 5, 6.5, 7.5, 9), contact time (30, 60, 90, 120, and 180 min), and bead biomass concentration (0.5, 1, 1.5, 2, and 3 g/L). Control experiments were performed using sodium alginate beads without *Scenedesmus regularis* biomass in the ZnO NPs solution[23]. To determine the adsorption equilibrium time, kinetic experiments were performed by collecting 0.5 mL samples at specific intervals and analyzing their concentrations using ICP-MS after appropriate dilution. Adsorption equilibrium tests were conducted in a shaking incubator, in which a predetermined amount of biomass was mixed with the ZnO NPs solution and agitated at 160 rpm for the established equilibrium time. These tests were repeated at different temperatures to assess the effect of temperature on adsorption. The initial *p*H of the solution was adjusted using NaOH and HCl. Following the adsorption process, the solution was filtered using Whatman filter paper before concentration analysis by ICP-MS to ensure accurate measurements of the remaining ZnO NPs in solution.

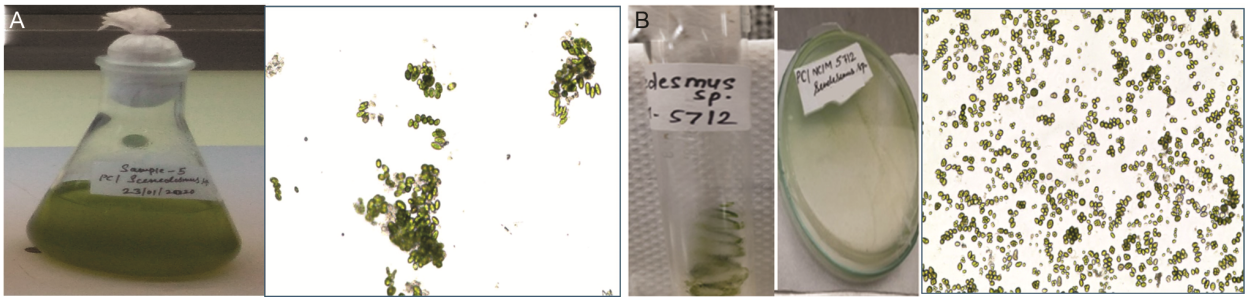

Fig. 2 — (A) Cells and colonies of *Scenedesmus regularis* isolates as observed under inverted microscope at 40× magnification; (B) Reference strain of *Scenedesmus* sp. NCIM-5712 and Cells of *Scenedesmus regularis* NCIM-5712 observed under inverted microscope at 40× magnification

$$\text{Removal efficiency} = \frac{\text{Ci} - \text{Cf}}{\text{Ci}} \times 100$$

[Where, C_i is the initial metal ion conc. (mg/L), C_f is the final (residual) metal ion conc. (mg/L)]

Characterization of biosorbent (biomass) before and after biosorption

The characterization of *Scenedesmus regularis* biomass before and after the biosorption experiment was performed using FTIR spectroscopy (Perkin Elmer, Spectrum Two) and SEM-EDX (Scanning Electron Microscope coupled with Energy Dispersive X-ray Detector) analyses. FTIR spectroscopy was performed to analyze the *Scenedesmus regularis* biomass samples before and after ZnO NPs biosorption[24]. This analysis aimed to detect any differences in functional groups on the *Scenedesmus regularis* biomass due to the interaction with ZnO NPs during the biosorption process. SEM was employed to verify topographical differences between the *Scenedesmus regularis* biomass before and after biosorption of ZnO NPs. This technique provides visual evidence of surface morphology changes. EDX analysis was conducted to identify the types of elements present in the sample and confirm the presence of ZnO NPs attached to the cell surface of *Scenedesmus regularis* biomass. This analysis offers elemental composition information, confirming the presence of zinc and oxygen atoms characteristic of ZnO nanoparticles.

Statistical analysis

The experimental data set for the biosorption of ZnO nanoparticles onto immobilized *Scenedesmus regularis* biomass was presented as the mean ± standard deviation (SD) from three replicates. Differences between the concentrations of ZnO nanoparticles before and after biosorption were analyzed using a single factor (one-way) analysis of variance (ANOVA) method, with three repetitions in each treatment. Results were considered statistically significant at $P < 0.05$ ($\alpha = 0.05$).

Results

Morphological & Molecular Characterization

The isolated *Scenedesmus* sp. exhibits oval cells and lacks thorn structures. These cells are organized into colonies of four or eight cells (Fig. 2)[25]. Each cell within these colonies falls in the range of 3.73-4.64 µm (Fig. 1 & 2). Morphological identification confirms that these isolates are closely related to the genus Scenedesmus. Positive confirmation of the presence of the *Scenedesmus regularis* microalgal species was achieved using the reference strain *Scenedesmus* sp. NCIM-5712 as a positive control.

Physical characteristics may vary in relation to the time and culture condition of microalgae present in all nearby ground ecosystems so molecular study is very significant to authentication microalgal species. The isolated sample was confirmed as *Scenedesmus regularis* by PCR followed by sequencing of amplified gene product (1061 bp) of 18S rRNA (Fig. 3).

Characterization of zinc oxide nanoparticles

UV-Vis results of zinc oxide nanoparticles

The UV-visible absorbance spectra of the synthesized ZnO nanoparticles are depicted in Fig. 4. The absorbance within the wavelength range of 200-600 nm was observed using UV-vis spectroscopy. A broad absorption peak of zinc oxide nanoparticles exhibited surface plasmon resonance spectra around 352 nm, confirming the successful synthesis of ZnO NPs.

FTIR spectrum of zinc oxide nanoparticles

The FTIR spectrum of zinc oxide NPs were obtained in the range of 4000-450 cm^{-1} using direct method at room temperature. Characteristic peaks of

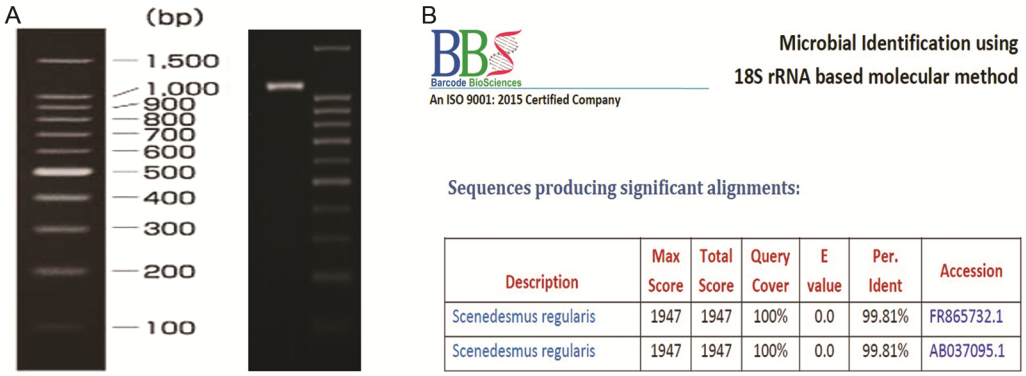

Description	Max Score	Total Score	Query Cover	E value	Per. Ident	Accession
Scenedesmus regularis	1947	1947	100%	0.0	99.81%	FR865732.1
Scenedesmus regularis	1947	1947	100%	0.0	99.81%	AB037095.1

Fig. 3 — (A) Polymerase Chain Reaction (PCR; (B) Sequencing result image of *Scenedesmus regularis*

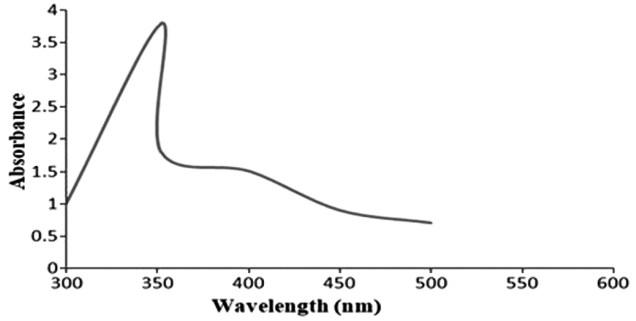

Fig. 4 — UV-Visible spectra of ZnO nanoparticles

ZnO showed at 3574.68, 3471.14, 1637.25, 1368.65, 1014.04, 885.38, 838.36 and 463.04 cm^{-1}. The FTIR spectra 3574.68 cm^{-1} exhibited a sharp peak in higher energy region due to O-H stretching presence of alcohols. The N-H stretching shows the presence of primary amine, the vibration bond arises at 3471.14 cm^{-1}. The FTIR spectra exhibited the strong, medium peak region at 1637.25, 885.38, 838.36 cm^{-1}. They represent C=C stretching alkene. The S=O stretching depicts the presence of sulfonamide, the vibration bond at 1368.65cm^{-1}. The C-F stretching showed the presence of fluoro compound, and the vibration bond arose at 1014.04 cm^{-1} [26]. The sharp peak positioned at 463.04 cm^{-1} is attributed to the presence of Zn-O stretching bonds[27]. All peaks are shown in Fig. 5 and also summarized in Table 1.

XRD analysis of zinc oxide nanoparticles

The powder X-ray diffraction pattern (XRD) obtained by zinc oxide nanoparticles is shown in Fig. 6. The characteristic XRD peaks with 2 theta values of 31.67°, 34.32°, 36.11°, 47.40°, 56.41°, 62.75°, 67.79°, and 76.82° correspond to the Miller Indices (hkl) values (crystal plans) (100), (002), (101), (102), (110), (103), (112), and (202) showing resemblance with the reference JCPDS file No. 75-0592[21]. The average crystallite size of ZnO NPs was evaluated by using the "Debye-Scherrer′s equation". The calculated average particle size is approximately 29.97 nm.

TEM analysis of zinc oxide nanoparticles

Transmission electron microscopy (TEM) analysis was conducted to determine the exact size and morphology of the synthesized zinc oxide nanoparticles (ZnO NPs). Fig. 7A illustrates that the size of the ZnO NPs ranged from 20 to 30 nm, as observed from TEM imaging. Fig. 7B presents the selected area diffraction pattern (SAED) of the ZnO nanoparticles, confirming that the particles are well crystallized.

Immobilization of *Scenedesmus regularis* microalgal biosorbent (biomass)

Sodium alginate beads (4%) were prepared with optimized biosorbent concentrations of dried *Scenedesmus regularis* microalgal biomass and prepared control beads of sodium alginate without incorporation of the *Scenedesmus regularis* microalgal biomass (Fig. 8)

Batch sorption study

Influence of pH

The *p*H of the solution containing ZnO nanoparticles (NPs) varied between 4.0 and 9.0, while the values of other experimental parameters were kept constant. It was observed that as the *p*H increased from 4 to 6.5, the biosorption capacity also increased[28] (Fig. 9). However, when the *p*H was further increased to 9.0, the percentage of ZnO NPs removal by the immobilized *Scenedesmus regularis* biomass did not change significantly. At lower *p*H levels, the solubility and mobility of metal ions increase. Zinc is predominantly present in the solution in cationic forms at *p*H 6.0. Therefore, the *p*H of the water in the present experiment was adjusted to 6.5 before contact with the immobilized *Scenedesmus*

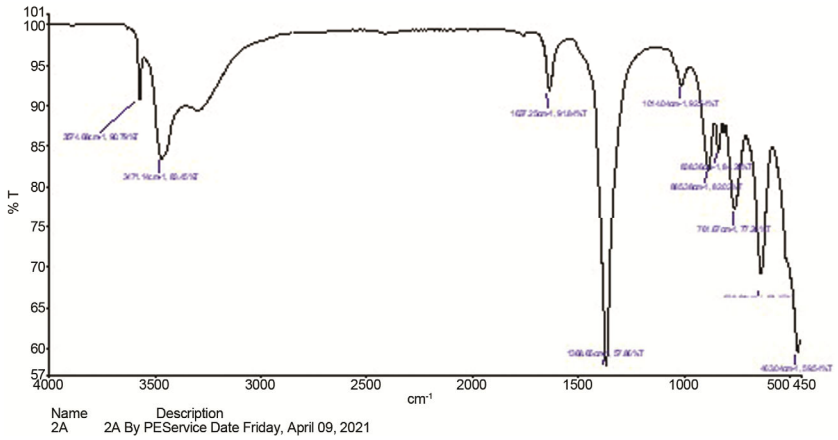

Fig. 5 — FTIR spectrum of chemically synthesized ZnO NPs showing functional groups

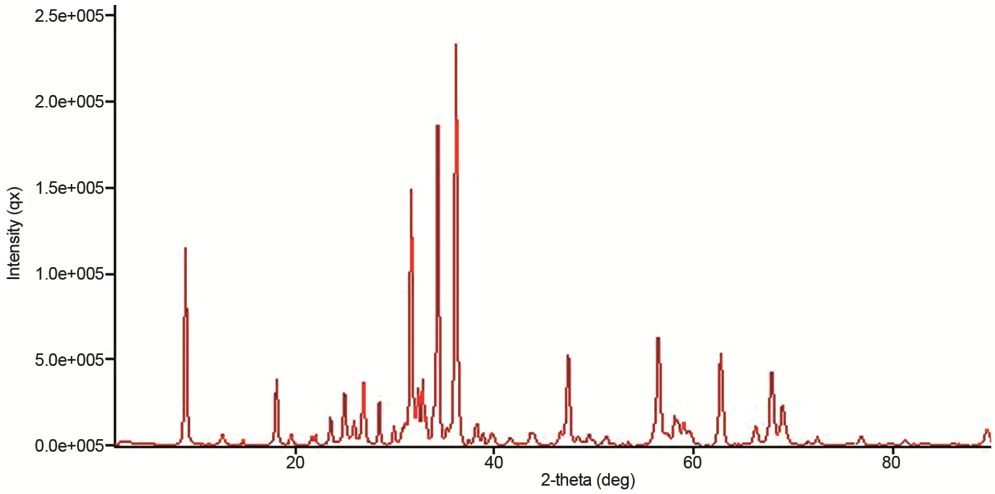

Fig. 6 — X-ray diffraction patterns of zinc oxide nanoparticles

Table 1 — Possible assignments of FTIR spectra for ZnO Nanoparticles

Frequency (cm-1) ZnO NPs	Bond type	Bond Origin	Possible functional group
3574.68	Sharp	O-H Stretching	Alcohol (free)
3471.14	Strong, Medium	N-H Stretching	Alcohol (Intermolecular), Primary amine
1637.25		C=C Stretching, N-H Bending, C=C	
885.38	Medium, Strong	Stretching,	Conjugated alkane, Amine, Alkene, 1,2,4-
838.36		C-H Bending	trisubstituted
1368.65		C-H Bending, O-H Bending, O-H Bending,	
	Medium, Strong	S=O Stretching	Alkene, Alcohol, Phenol, Sulfonate, Sulfonamide
1014.04	Strong, Medium	C-F Stretching, C-O Stretching, C-N Bending	Fluoro compound, Alkyl aryl ether, Amine, Vinylether
463.04	Strong	Zn-O Stretching	

regularis. This slight acidification may enhance the solubility of ZnO NPs and their bioavailability to the *Scenedesmus regularis* beads. However, at *p*H above 7.0, the solubility of zinc decreases, and the presence of cationic forms drastically diminishes. Consequently, the uptake of zinc oxide NPs was not high under these conditions. The removal efficiency of ZnO nanoparticles increased significantly from 12.2% to 82.53% when using 2 g/L immobilized *Scenedesmus regularis* biosorbents, indicating that the

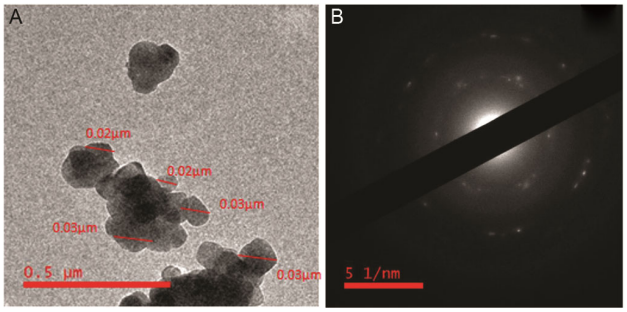

Fig. 7 — (A) TEM Micrograph; (B) SAED Pattern of synthesised ZnO nanoparticles

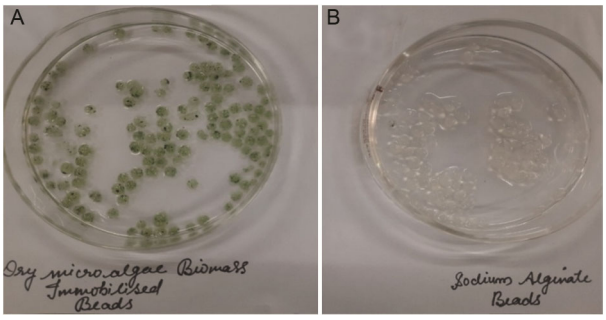

Fig. 8 — (A) Immobilization of dried *Scenedesmus regularis* microalgal biomass in alginate beads and its application in ZnO NPs removal from aqueous solution; (B) Sodium alginate beads without incorporation of the *Scenedesmus regularis* microalgal biomass

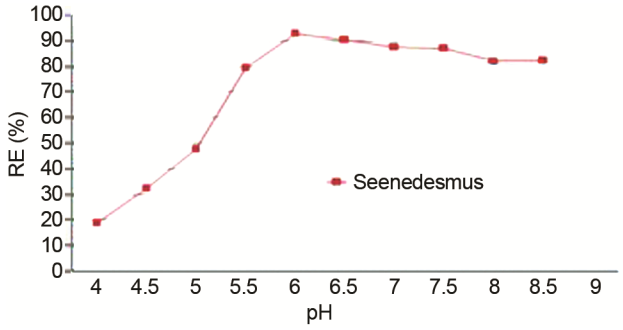

Fig. 9 — Effect of pH on removal of ZnO NPs from aqueous solution using 2g/L immobilized *Scenedesmus regularis* at 180 min contact time.

optimum *p*H for ZnO nanoparticles was 6.0[29]. However, the biosorption process decreased with any further increase in *p*H (> 6.5). This suggests that pH 6.0 is the most favorable condition for the biosorption of ZnO nanoparticles by immobilized *Scenedesmus regularis*, and deviations from this *p*H level result in decreased efficiency.

Influence of biosorbent dose

Batch experiments were conducted using different biosorbent doses (0.5, 1, 1.5, 2, and 3 g/L of test

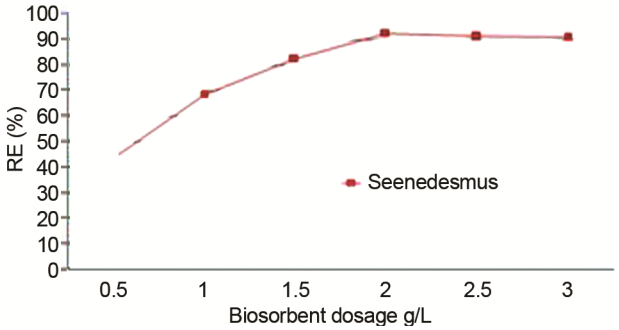

Fig. 10 — Effect of biosorbent dosage on percentage removal of ZnO NPs with immobilized *Scenedesmus regularis* biosorbents at *p*H 6.0 with 180 min contact time

Table 2 — Removal capacity (mg g^{-1}) and Removal efficiency (%) of immobilized *Scenedesmus regularis* beads for ZnO NPs removal at different times

Contact time (min)	ZnO nanoparticles removal	
	RC (mg g^{-1})	RE (%)
30	22.0	53.01
60	28.5	68.67
120	33.5	80.72
180	38.5	82.53
240	29.5	71.08

[RC-Removal capacity; RE-Removal Efficiency]

solution) to assess their effect on the uptake of ZnO nanoparticles. Fig. 10 illustrates that the uptake efficiency of ZnO nanoparticles increased from 37.8% to 82.53% as the biosorbent dosage of *Scenedesmus regularis* increased from 0.5 g/L to 2 g/L. The maximum biosorption efficiency of 82.53% was achieved with a *Scenedesmus regularis* biosorbent concentration of 2 g/L, indicating its effectiveness in removing ZnO nanoparticles from aqueous solutions.

Influence of contact time

The maximum uptake of ZnO nanoparticles occurred during 180 min of contact, recording 82.53% for immobilized *Scenedesmus regularis* beads (Table 2). As the exposure time was increased to 240 min, the percentage of ZnO NPs uptake gradually decreased until equilibrium was established between the percentage of ZnO NPs removal by immobilized *Scenedesmus regularis* cells and the concentration of the ZnO NPs in the external solution. After attaining equilibrium at 180 min, the available binding sites on the cell surface were occupied completely and no further uptake was observed[30]. Non-adsorbed free Zn ions formed compounds that decreased the efficiency of biosorption, as they cannot be associated with the amine group of the biomass. As a result, H^+ gets released into the solution and *p*H is reduced[31]. Due to the smaller size

of the released H^+ than Zn ions, their competition could be a reason of the desorption that occurs after time longer than the equilibrium value (180 min)[31].

Influence of nanoparticles concentration

The biosorption of ZnO nanoparticles had increased with the increasing concentration of ZnO NPs from 0.5 mg/L to 2 mg/L in the presence of immobilized *Scenedesmus regularis* microalgal beads. They removed the maximum percentage of 82.53% at 1.66 mg/L concentration. It indicated that biosorption was even favorable for the higher initial NPs concentration. Metal ions concentration plays vital role on biosorption. Omar *et al*. confirmed that zinc uptake by microalgae increased with increasing concentration of metal ions[32].

ICP-MS

Using the optimized conditions, experiments were conducted to investigate the abilities of immobilized *Scenedesmus regularis* microalgal biomass in sodium alginate beads to remove ZnO NPs in aqueous medium. The analysis was performed using ICP-MS, and the experimental data were subjected to a single factor/one-way analysis of variance (ANOVA) method with three repetitions in each treatment. Results were considered significant at $P < 0.05$. Mean and standard deviation were calculated from the data obtained from ICP-MS analysis to obtain a representative average. Laboratory scale conditions of for the immobilization of ZnO nanoparticles using *Scenedesmus regularis* microalgal biomass in sodium alginate beads were optimized. The results indicated that immobilized *Scenedesmus regularis* microalgal biomass in sodium alginate beads was effective in removing 82.53% of ZnO NPs at an initial concentration of 1.66 mg/L for 3 h.

Characterization results of *Scenedesmus regularis* microalgal biosorbent (biomass) before and after biosorption

FTIR (Fourier transform infrared)

The FTIR spectrum for the microalgal biomass sample treated with ZnO NPs showed several changes in the characteristic absorption peaks, indicating that these functional groups are involved in biosorption (Fig. 11 & Table 3). The control spectrum of

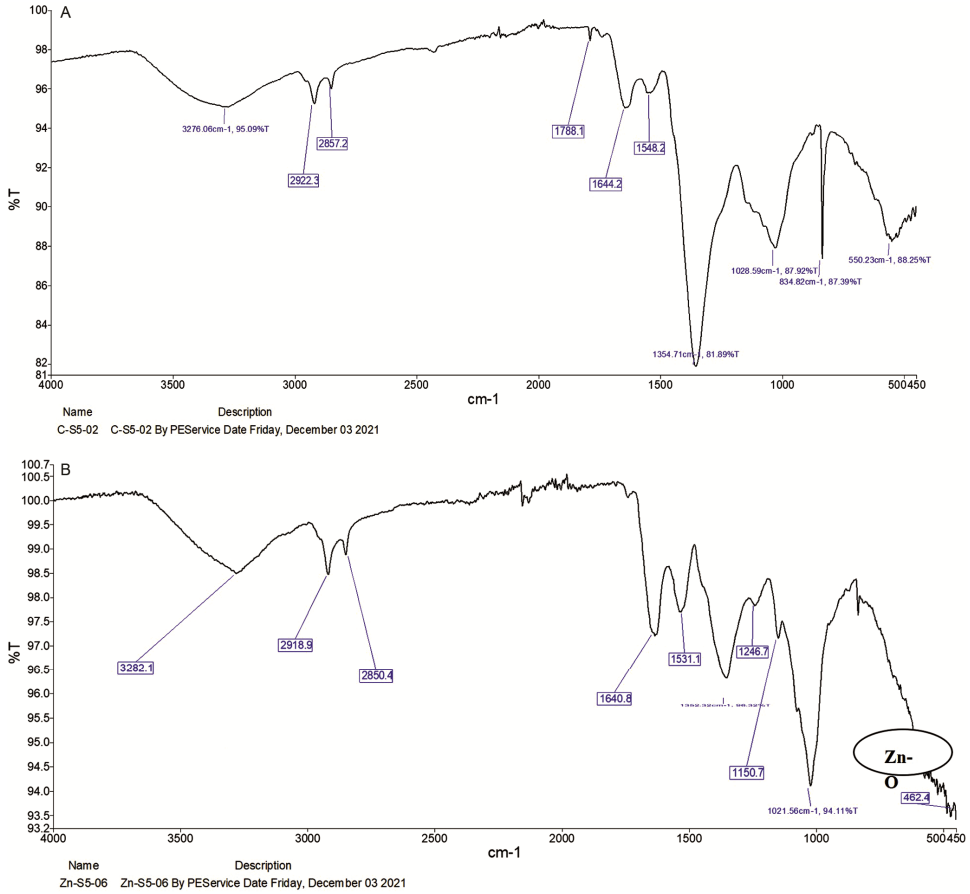

Fig. 11 — FTIR spectrum of *Scenedesmus regularis* biomass (A) before ZnO NPs biosorption; (B) after ZnO NPs biosorption from aqueous solution

Table 3 — FTIR spectra of *Scenedesmus* regularis microalgal biomass before and after ZnO NPs biosorption

Wave number range (cm^{-1})	Before ZnO NPs biosorption		After ZnO NPs biosorption		Difference
	Wave number (cm^{-1})	Bond Origin	Wave number (cm^{-1})	Bond Origin	
3029-3639	3276.06	O-H stretching, N-H stretching(Amide)	3282.1	O-H stretching N-H stretching(Amide)	-6.04
2809-3012	2922.3	Lipid-carbohydrate C-H stretch	2918.5	Lipid-carbohydrate C-H stretch	3.8
1583-1709	1644.2	N-H band C=O stretching	1640.8	N-H band C=O stretching	3.4
1191-1356	1354.71	Nucleic acid P=O stretching	1352.32	Nucleic acid P=O stretching	-2.39
980-1072	1028.59	C-O-C polysaccharides Carbohydrate	1021.58	C-O-C polysaccharides Carbohydrate	-7.01
821.-708	834.82	Si-OH group	-	-	-
484-559	550.23	PH Phosphine group	462.4	Zn-O	-

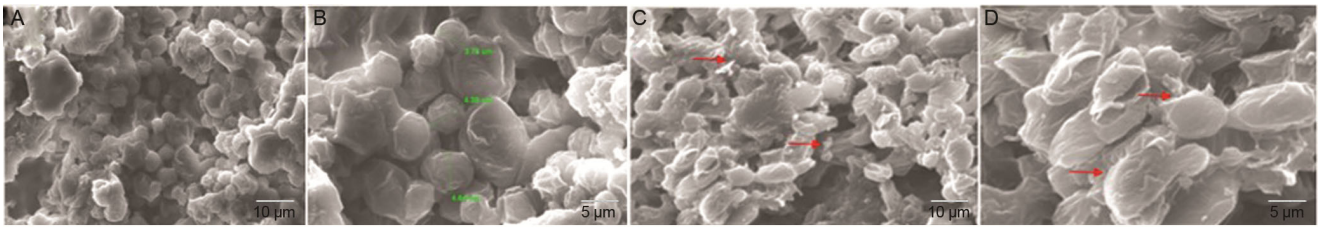

Fig. 12 — SEM micrograph of *Scenedesmus regularis* biomass (A&B) before and (C&D) after ZnO NPs biosorption from aqueous solution

uninteracted biomass (not treated with ZnO NPs) displayed a peak at 3276.06 cm^{-1}, representing the presence of hydrogen-bonded O-H stretch. Peaks at 1354.71 cm^{-1} and 1028.59 cm^{-1} were attributed to the nucleic acid P=O stretching of phosphodiesters and C-O-C carbohydrates, respectively. The peak at 833.82 cm^{-1} indicated the presence of a phosphine group, and the peak at 550.23 cm^{-1} represented the Si-OH group[33]. In contrast, the treated biomass with ZnO NPs exhibited a peak at 3282.1 cm^{-1}, representing the hydrogen-bonded O-H stretch. A peak at 2918.5 cm^{-1} indicated the presence of a C-H stretch. The peak at 1640.8 cm^{-1} showed the vibration of N-H from a primary amine. The peaks at 1302.32 cm^{-1} and 1021.56 cm^{-1} were due to the stretching vibrations of P=O and C-O-C, respectively. Additionally, a peak at 462.4 cm^{-1} was associated with the stretching vibration of ZnO[34]. These changes in the wave number and their intensity were a result of the interaction between the functional groups on the Scenedesmus biomass and ZnO NPs during the biosorption process.

SEM (Scanning electron microscopy)

SEM was used to verify the morphological differences between the *Scenedesmus regularis* microalgal biomass before and after biosorption of ZnO nanoparticles. Fig. 12 presents SEM micrographs of *Scenedesmus regularis* biomass before and after the adsorption of ZnO NPs. The SEM images confirmed the presence of ZnO-NPs on the *Scenedesmus regularis* microalgae cell surface (Fig. 12C). The SEM images in Fig. 12A & 12B illustrated typical untreated cells with intact and rigid cell walls. The size of this microalga was in the range of 3.73 µm to 4.64 µm. After ZnO-NPs biosorption, the cell wall of the biomass was distorted, exhibiting an irregular surface with the appearance of bright spots due to the accumulation of ZnO NPs (Fig. 12C & 12D). The red arrows indicated the attachment of ZnO nanoparticles onto the algal cell wall of *Scenedesmus regularis* after biosorption (Fig. 12C & 12D).

EDX (Energy dispersive X-Ray)

Energy-dispersive X-ray spectroscopy (EDX) is a useful tool for chemical characterization and

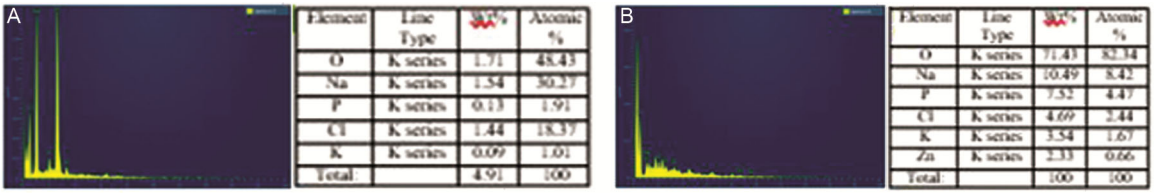

Element	Line Type	Wt%	Atomic %
O	K series	1.71	48.43
Na	K series	1.54	30.27
P	K series	0.13	1.91
Cl	K series	1.44	18.37
K	K series	0.09	1.01
Total:		4.91	100

Element	Line Type	Wt%	Atomic %
O	K series	71.43	82.34
Na	K series	10.49	8.42
P	K series	7.52	4.47
Cl	K series	4.69	2.44
K	K series	3.54	1.67
Zn	K series	2.33	0.66
Total:		100	100

Fig. 13 — EDX analysis for *Scenedesmus regularis* microalgal biomass (A) before and (B) after ZnO NPs biosorption from aqueous solution

elemental analysis of biomass. In the present study, EDX analysis was performed to determine the types of elements present in the sample and to confirm the presence of ZnO nanoparticles attached to the cell surface of *Scenedesmus regularis* microalgal biomass. In Fig. 13, the EDX spectra revealed the elemental composition of *Scenedesmus regularis* biomass before and after the biosorption of ZnO nanoparticles. According to the spectra, the untreated biomass contained elements such as oxygen (O), sodium (Na), phosphorus (P), chlorine (Cl), and potassium (K). After the biosorption process, the EDX analysis results indicated a significant increase in the percentage of oxygen, rising from 48.43 wt% to 82.32 wt% of the total weight. This increase in oxygen content is consistent with the presence of ZnO nanoparticles, which contribute additional oxygen atoms to the biomass. Distinct peaks corresponding to the zinc (Zn) atoms were also observed, confirming the presence of ZnO nanoparticles. The elemental profile showed a strong peak at 1 KeV, characteristic of Zn, and an oxygen peak centered at 0.5 KeV. These peaks are indicative of ZnO and align with the expected energy levels for these elements[35,36]. The results from the EDX analysis clearly demonstrated the presence of ZnO nanoparticles in the *Scenedesmus regularis* biomass after biosorption, compared to the control sample which did not contain ZnO nanoparticles. This confirms that the biosorption process was effective in incorporating ZnO nanoparticles into the microalgal biomass.

Discussion

The present study focuses on the uptake of zinc oxide (ZnO) nanoparticles using immobilized *Scenedesmus regularis* green microalgae. Isolated green microalgal samples showed similarity to the genus Scenedesmus based on morphological characterization[37]. Species-level identification was achieved through PCR and 18S rRNA gene sequencing, with nucleotide sequences obtained from Barcode Biosciences, Bengaluru, Karnataka[38]. The synthesis of ZnO nanoparticles was confirmed by the colour change from colourless zinc nitrate to white precipitate, indicating that a reaction had occurred and particles had formed[17]. The FTIR spectrum of zinc oxide (ZnO) nanoparticles showed high stretching of alcohols, primary amine, strong medium stretching of alkene, stretching of sulfonamide, and stretching of fluoro compounds. Similar findings were reported by Sunajadevi & Sugunan, Nithya & Kalyanasundharamb, and Shanmugapriya *et al*.[26,27]. The UV-Vis spectra around 352 nm confirmed the successful synthesis of ZnO nanoparticles. Previous studies support these UV-Vis results, indicating a characteristic peak near 352 nm corresponding to the intrinsic band-gap absorption of ZnO. X-ray diffraction (XRD) results showed a crystal lattice peak at (002), confirming that the ZnO nanoparticles formed are pure ZnO with a wurtzite hexagonal structure, as compared with data from the JCPDS-ICDD card: 75-0592[26]. The average crystallite size of ZnO nanoparticles was evaluated using the Debye-Scherrer equation, with a calculated average particle size of approximately 29.97 nm. Transmission electron microscopy (TEM) techniques further proved that all particles had a crystallographic structure within the nano-range.

Biosorption optimization results showed that biosorption of nanoparticles by microalgal biomass is dependent on *p*H. *p*H influences the functional groups on the cell surface and metal ions form in the solution. The microalgae cell wall contains alginate that facilitates absorption properties due to presence of carboxyl and hydroxyl groups[10]. Farooq *et al.* have explained that decreased biosorption of metal ions at higher *p*H may be due to the precipitation of metals in the metal hydroxide form. Alternatively, when *p*H value is low, the H^+ concentration is high, that will competitively exchange cations on the algal surface[39]. In contrast, many researchers found in previous studies that the uptake efficiency was strongly related to the biosorbent dosage like *p*H. *p*H plays a crucial role in biosorption as it influences the surface charge

of the biosorbent. The zero point charge (ZPC) refers to the *p*H at which the surface charge of the material is neutral (neither positive nor negative). If the *p*H is greater than the ZPC, the surface becomes negatively charged, as the biosorbent will have more deprotonated functional groups (such as carboxyl or hydroxyl groups). If the *p*H is lower than the ZPC, the surface becomes positively charged, as more protonation of functional groups occurs, making the surface attract anions (e.g., ZnO nanoparticles) more effectively. In general, it can be accomplished that a higher dose of biosorbent significantly increases the uptake percentage because more functional groups and surfaces were available on the biosorbent with which the metals could interact easily. Electrostatic interactions between algal cells may function as a momentous factor in association between biomass dosage and metal biosorption[30,40]. The metal ion concentration also plays a vital role in biosorption. The algal cell wall shows the highest adsorption efficiency at lower concentrations, and increases in the metal ion concentrations lead to decreased adsorption efficiency due to saturation of adsorbent sites on microalgal cell wall. Mingzhong *et al*. reported, an aqueous solution with a higher metal concentration contains additional metal ions around the biosorbent active sites where metal ions would be adsorbed more adequately[41]. The kinetic rate of biosorption depends on the assurance of contact time. The biosorbent gets to be saturated with the nanoparticles. As contact time increases the desorption process may also start. The biosorption and desorption rates reach an equilibrium point. The biosorbent will not bind to the biomass after the biosorption process accomplishes equilibrium condition[42].

Batch sorption studies confirmed that the maximum biosorption of ZnO nanoparticles (ZnO NPs) was 82.53% using immobilized *Scenedesmus regularis* biomass in sodium alginate beads. This maximum biosorption was achieved under the following optimum operating conditions: an initial ZnO concentration of 1.66 mg/L, a temperature of 37°C, a pH of 6.0, a biomass concentration of *Scenedesmus regularis* at 2 g/L, and a contact time of 180 min. The binding mechanisms between ZnO nanoparticles (ZnO NPs) and the *Scenedesmus regularis* green microalgae surface can be inferred from the shifts and changes in the FTIR peaks observed before and after adsorption. The adsorption process is likely driven by a combination of electrostatic interactions, hydrogen bonding, and coordination between Zn ions and functional groups (such as hydroxyl, carboxyl, amine, and sulfonate) present on the algal cell wall. These interactions facilitate the attachment of ZnONPs onto the microalgal surface. O-H/N-H Stretch (3276.06 cm^{-1} to 3282.1 cm^{-1}): The shift in the broad peak indicates the involvement of hydroxyl (-OH) and amine (-NH) groups in the binding process. These functional groups likely form hydrogen bonds or coordinate with ZnO NPs; C-H Stretch (2922.3 cm^{-1} to 2918.5 cm^{-1}): The slight shift in the C-H stretching vibration suggests weak interactions, such as Van der Waals forces, between the algal surface and ZnO NPs; C=O Stretch in Amides (1644.2 cm^{-1} to 1640.8 cm^{-1}): The shift in the carbonyl peak implies the participation of amide or carboxyl groups in binding ZnO NPs, possibly through coordination with zinc ions; C-N and O-H Bending (1354.71 cm^{-1} to 1352.32 cm^{-1}): The shift suggests that amine or hydroxyl groups are involved in the adsorption, likely through electrostatic or covalent interactions with ZnO NPs; C-O Stretch (1028.59 cm^{-1} to 1021.58 cm^{-1}): The shift in this region indicates the involvement of hydroxyl and possibly sulfonate or sulfate groups in the biosorption process, forming bonds with ZnO NPs; Disappearance of peak at 834.82 cm^{-1} and emergence at 462.4 cm^{-1}: The disappearance of the peak at 834.82 cm^{-1}, related to Zn-O bonding, and the new peak at 462.4 cm^{-1}, possibly indicating new Zn-O bonds, suggests that ZnONPs formed direct interactions with the algal cell wall.

The high content of lipids, nucleic acids, and carbohydrates provides the major biosorption sites for ZnO binding. SEM images confirmed the attachment of ZnO nanoparticles to the *Scenedesmus regularis* cell surface. The SEM images showed untreated cells with intact and rigid cell walls, while treated cells exhibited distorted cell walls with irregular surfaces and bright spots due to ZnO NP accumulation. EDX analysis further confirmed the presence of Zn elements in the sample, indicating successful attachment of ZnO NPs to the *Scenedesmus regularis* biomass. The elemental profile showed a strong peak at 1 KeV characteristic of Zn and an oxygen peak centered at 0.5 KeV.

Based on these results, the immobilized *Scenedesmus regularis* microalgal biomass in sodium

alginate beads was effective in removing ZnO nanoparticles. Additionally, this biosorbent has the potential to be reused for multiple cycles of nanoparticles uptake, demonstrating its efficiency and sustainability in ZnO NPs removal from aqueous solutions.

Conclusion

The outcomes of this study demonstrate that immobilized *Scenedesmus regularis* in sodium alginate beads is effective in the removal of ZnO nanoparticles and has the potential to be reused for multiple cycles of nanoparticles uptake. The removal efficiency was 82.53%. Data suggests that *Scenedesmus regularis* green microalgae could be used as a promising, efficient, cheap, and biodegradable biomass for ZnO nanoparticles removal. This research can be valuable to industries searching for efficient, simple, and green alternatives for nanoparticles treatment methods.

Acknowledgements

Authors wish to express our sincere acknowledgment to Dr. Ashok Kumar Chauhan, President, RBEF parent organization of Amity University Madhya Pradesh (AUMP), Gwalior, Dr. Aseem Chauhan, Additional President, RBEF and chairman of AUMP, Gwalior, Lt. Gen. V.K. Sharma, AVSM (Retd.), Pro Chancellor of AUMP, Gwalior for providing necessary facilities, their Valuable support and encouragement throughout the work. The authors also express their sincere thanks to the Central Instrumentation facilities at Jiwaji University, Gwalior, and DST-SAIF Cochin, at Kochi, Kerala, India for Characterization facilities availed.

Conflict of interest

The authors have no conflict of interest to declare.

References

1 Shrivastava N, Shrivastava V, Tomar RS, & Jyoti A, Toxic effects of Copper Oxide nanoparticles on *Chlorella vulgaris*. *Internat Journ of Environ Heal Eng*, 13(2024) 1.

2 Mehennaoui K, Cabier S, SerchiT, Ziebel J, Lentzen E, &Valle N, Do the pristine physic-chemical properties of silver and gold nanoparticles influence uptake and molecular effects on *Gammarus fossarum* (Crustacea Amphipoda)? *Sci of the Tot Environ*, 643(2018)1200.

3 Wu M, Li Y, Yue R, Zhang X, & Huang Y, Removal of silver nanoparticles by mussel-inspired Fe3O4@ polydopamine core-shell microspheres and its use as efficiency catalyst for methylene blue reduction. *Sci Rep*, 7(2017) 1.

4 Zhang C, Hu Z, & Deng B, Silver nanoparticles in aquatic environments: Physiochemical behavior and antimicrobial mechanisms. *Wat Res*, 88 (2016) 403.

5 Khan I, Saeed K, & Khan I, Nanoparticles: Properties, applications and toxicities. *Arab Jour of Chem*, 12 (2019) 908.

6 Cheng HH, Chen SS, Liu HM, Jang LW, & Chang SY, Glycine-Nitrate combustion synthesis of Cu-based nanoparticles for NP9EO degradation applications. *Catalyst*,10 (2020) 1061.

7 Azimi A, Azari A, Rezakazemi M, & Ansarpour M, Removal of heavy metals from industrial wastewater: a review. *Chem Bio Eng Reviews*, 4(2017) 37.

8 Shrivastava N, Shrivastava V, Jyoti A, & Tomar RS, Promises and Cons of Nanobiotechnology-A Critical Review. *Plant Arch*, 19 (2019) 1.

9 Cheng K, Qu L, Mao Z, Biosorption of thorium onto *Chlorella Vulgaris* microalgae in aqueous media. Sci Rep 14 (2024)20866.

10 Udaiyappan AFM, Hasan HA, Takriff MS, & Abdullah SRS, A review of the potential, challenges and current status of microalgae biomass applications in industrial wastewater treatment. *J Water Process Eng*, 20 (2017) 8.

11 Srinuanpan S, Cheirsilp B, & Kassim MA, Oleaginous microalgae cultivation for biogas upgrading and phytoremediation of wastewater. In *Microalgae cultivation for biofuels production.* Editor A. Yousuf (Cambridge, Massachusetts; Elsevier Academic Press), (2020) 69.

12 Sumiahadi A, &Acar R, A review of phytoremediation technology: heavy metals uptake by plants. *IOP Conference Series: Ear and Environ Sci*. (2018) 142.

13 Dhanapal AR, Thiruvengadam M, Vairavanathan J, Venkidasamy B, Easwaran M, Ghorbanpour M. Nanotechnology Approaches for the Remediation of Agricultural Polluted Soils. *ACS Omega*, 13(2024)13522.

14 Apandi N, Mohamed, RMSR, Al-Gheethi, A. et al. Scenedesmus biomass productivity and nutrient removal from wet market wastewater, A bio-kinetic study. *Waste Biomass Valor* 10, (2019), 2783.

15 Anyanwu R.C, Rodriguez C, Durrant A, and Olabi A.G, Evaluation of growth rate and biomass productivity of *Scenedesmus quadricauda* and *Chlorella vulgaris* under different LED wavelengths and photoperiods. Sustainability, 14(2022), 6108.

16 Hamadamin SI, Anwer SS, Abdulkareem PM, & Sdiq KH, Biogenic synthesis of ferrous (III) oxide and Fe_3O_4/SiO_2using *Chlorella* sp. and its adsorption properties of water contaminated with copper (II) ions. *Bull Chem Soc*, 36 (2022) 585.

17 Mourdikoudis S, Pallares RM, &Thanh NTK, Characterization techniques for nanoparticles: comparison and complementarity upon studying nanoparticles properties. *Nanoscale*, 10 (2018) 12871.

18 Shrivastava N, Shrivastava V, Tomar RS, & Jyoti A, Toxic Effects of Zinc Oxide Nanoparticles to *Scenedesmus quadricauda* Microalgae. *Bull of Environ, Pharmacol and Life Sci*. 3 (2022) 253.

19 Al-Selwey WA, Ibrahim AA, Labis JP, & Seleiman MF, Effects of Zinc Oxide and Silicon Dioxide nanoparticles on physiological, yield, and water use efficiency traits of potato grown under water deficit. *Plants (Basel)*,12 (2023) 218.

20 Zaharieva MM, Dimitrova DZ, Videva SR, IIieva Y, Brachkova A, &Balabanova V, Antimicrobial and Antioxidant potential of *Scenedesmus obliquus* microalgae in the context of integral biorefinery concept. *Molecule*, 277 (2022)519.

21 Dan H, Jiaxing Z, Ruoyu C, Zhihong Y, Jiangjun H, & Yohanes KN, Microalgae *Chlorella vulgaris* and *Scenedesmus dimorphus* co-cultivation with landfill leachate for pollutant removal and lipid production. *Biores Technol*, 342 (2021) 126003.

22 Siwi WP, Rinanti A, Silalahi MDS, Hadisoebroto R, & Fachrul MF, Effect of immobilized biosorbents on the heavy metals (Cu^{2+}) biosorption with variations of temperature and initial concentration of Waste. *IOP Conf Series: Earth and Environ Sci* 106 (2018) 012113.

23 Lu WY Liang C, Musah BI, &Peng L, Simultaneous biosorption of Arsenic and cadmium onto chemically modified *Chlorella vulgaris* and *Spirulina platensis*. Water, 13(2021) 2498.

24 Syafiuddin A, Salmiati S, Hadibarata T, Salim MR, Kuehm ABH, & Suhartono S, Removal of Silver Nanoparticles from Water Environment: Experimental, Mathematical formulation, and Cost Analysis. *Water, Air & Soil Poll*, 230 (2019) 1.

25 Anyanwu RC, Rodrigue, C, Durrant A, & Olabi AG, Evalution of growth rate and biomass productivity of *Scenedesmus quadricauda* and *Chlorella vulgaris* under different LED wavelengths and photoperiods. *Sustainab*, 14 (2022) 6108.

26 Nithya K, &Kalyanasundharamb S, Effect of chemical synthesis compared to biosynthesized ZnO nanoparticles using aqueous extract of *C. halicacabum* and their antibacterial activity. *Open Nano* (2019) 4100024.

27 Shanmugapriya J, Monisha P, Nandini A, Praveena K, Synthesis of Zinc Oxide Particles from *Aloe baebadensis* for Medical Application. *Internat Journ of Eng Res & Technol*, 7 (2019).

28 Kumar SD, Santhanam P, Jayalakshmi T, Anantha S, & Nanda Kumar P, Optimization of pH and retention time on the removal of nutrients and heavy metal (zinc) using immobilized marine microalgae *Chlorella marina*. *Journ of Biol Sci*, 13 (2013) 400.

29 Monteiro CM, Castro PML & Malcata FX, Biosorption of zinc ions from aqueous solution by the microalga *Scenedesmus obliquus*. *Environ Chem Letter*, 19 (2011) 169.

30 Shalaby M.A, Matter I.A, Ghatieb M.M, Darwesh O.M, Biosorption performance of the multi-metal tolerant fungus Aspergillus sp. for removal of some metallic nanoparticles from aqueous solutions. Heliyon 9(2023) e16125.

31 Zareh M.M, El-Sayed A.S, El-Hady D.M, Biosorption removal of iron from water by Aspergillus niger. npj Clean Water, 5(2022) 58.

32 Olivera RH, Mata MT, &Valdes J, Riquelme C, Biosorption of Zn (II) from seawater solution by the microalgae Biomass of *Tetraselmis marina* AC16-MESO. *Int J Mol Sci* 22(2021) 12799.

33 Martin P, Carlos EO, &Funk C, Biosorption of Cd(II) by Nordic microalgae: Tolerance, Kinetics and equilibrium studies. *Algal Res*, 59 (2021)102471.

34 Manjunatha SS, &Girisha ST, Characterization of microalgal biomass through fourier transforms infrared (FTIR) spectroscopy. *Internat Jour of Bot Stud*, 6(2020) 57.

35 Al-Qasmi N, Facial Eco-Friendly Synthesis of Copper Oxide Nanoparticles Using Chia Seeds Extract and Evaluation of Its Electrochemical Activity. *Processes*, 9(2021) 2027.

36 Al-Kordy HMH, Sabry SA & Mabrouk MEM, Statistical optimization of experimental parameters for extracellular synthesis of zinc oxide nanoparticles by a novel haloalaliphilicAlkalibacillussp.W7. *Scient Rep*,11 (2021) 10924.

37 Tiara W, Nanda Astuti L, Ameli S, Rositayanti H, & Melati F, The biosorption of copper metal by tropical microalgae beads biosorbent. *Internat Jour of Scien & Technol Res*, 9 (2020) 3533.

38 Kumar S, Stecher G, Li M, Knyaz C, & Tamura K, MEGA X: Molecular evolutionary genetics analysis across computing platforms. *Mol Biol and Evol*, 35(2018) 1547-1549.

39 Farooq U, Kozinski J, Ain Khan M, Athar M, Biosorption of heavy metal ions using wheat based biosorbents-A review of the recent literature. Biores. Technol, 101(2020), 5043-5053.

40 Cheng K, Qu L, Mao Z, Biosorption of thorium onto *Chlorella Vulgaris* microalgae in aqueous media. Sci Rep 14 (2024)20866.

41 Mingzhong L, Hong J, & Ziaona L, (2021). Biosorption of $Cu^{2+,}$ $Pb^{2+,}$ Cd^{2+} and their mixture from aqueous solutions by *Micgelia figo* sawdust. Scientific reports, 11(2021), 11527.

42 Chen P, Wang B, Wu Y, Wang Q, Huang Z, Wang C, Urban river water quality monitoring based on self-optimizing machine learning method using multi-source remote sensing data. Ecol. Indic., 146(2023) 109750.